AERODYNAMIC INTERFERENCE BETWEEN EXHAUST SYSTEM AND AIRFRAME

by

Jack F. Runckel

Langley Research Center
National Aeronautics and Space Administration
Hampton, Virginia, USA

Presented at the AGARD Specialists Meeting on "Aerodynamic Interference"

Silver Spring, Maryland
September 28-30, 1970

SUMMARY

The purpose of this paper is to examine some mutual aircraft afterbody and engine nozzle interferences. Information was obtained from many model experimental investigations of jet interference obtained by the Langley Research Center at subsonic, transonic, and supersonic speeds. Emphasis is placed on studies of twin-engine fuselage configurations with nozzles installed near the terminus of the afterbody where the interactions of the nozzle exhausts and the external stream produce a complex flow-field environment. Airframe interferences on nozzle performance considered are: installation locations in the afterbody, boattailing ahead of the nozzles, and effects of tails and protuberances. Airframe interference on nozzle performance may be either detrimental or favorable, depending on the particular installation. Nozzle shape and jet exhaust interference can alter aircraft performance and stability. The effect on afterbody drag of nozzle exit axial location appears to pose more problems than the lateral spacing of the nozzles. For closely spaced nozzles, the shape of the interfairing between the nozzles has a pronounced effect on afterbody and nozzle performance.

NOTATION

A_{max}	maximum cross-sectional area of body
$C_{D,a}$	afterbody drag coefficient, $\frac{D_a}{q_\infty A_{max}}$
$C_{D,a+n}$	afterbody plus nozzle drag coefficient, $\frac{D_{a+n}}{q_\infty A_{max}}$
$C_{p,b}$	base pressure coefficient, $\frac{p_b - p_\infty}{q_\infty}$
$\bar{c}$	aircraft wing mean aerodynamic chord
D_a	drag force on afterbody
D_{a+n}	drag force on afterbody and nozzles
D_n	drag on nozzles
d_e	nozzle exit diameter
d_n	nozzle maximum diameter
d_t	nozzle throat diameter
F_i	ideal isentropic thrust of nozzles
F_j	measured jet (gross) thrust of nozzles
L	lift force
M	free-stream Mach number
M_Y	pitching moment about lateral axis
p_b	interfairing base static pressure
$p_{t,j}$	jet total pressure
p_∞	free-stream static pressure
q_∞	free-stream dynamic pressure
S	reference wing area
s	distance between engine center lines
α	model angle of attack, deg
β_a	afterbody boattail angle ahead of nozzle, deg
β_n	nozzle boattail angle, deg
ΔC_D	incremental aircraft drag coefficient due to jet operation, $\frac{D_{\text{jet on}} - D_{\text{jet off}}}{q_\infty S}$
ΔC_L	incremental aircraft lift coefficient due to jet operation, $\frac{L_{\text{jet on}} - L_{\text{jet off}}}{q_\infty A_{max}}$
ΔC_m	incremental aircraft pitching-moment coefficient due to jet operation, $\frac{(M_Y)_{\text{jet on}} - (M_Y)_{\text{jet off}}}{q_\infty \bar{c} S}$
$\frac{\Delta(F_j - D_n)}{F_i}$	ratio of incremental nozzle thrust minus drag to ideal thrust
δ_h	horizontal-tail deflection angle, deg

ABBREVIATIONS

AUG.	augmented power	C-D	convergent-divergent	F.R.	fineness ratio
B-I-D	blow-in-door	CONV.	convergent	MAX.	maximum

AERODYNAMIC INTERFERENCE BETWEEN EXHAUST SYSTEM AND AIRFRAME

1. INTRODUCTION

The resurgence of new military aircraft development has focused attention on the back end problem of airframe-engine nozzle integration. This area has become more critical because of requirements for multimission aircraft to operate effectively at subsonic, transonic, and supersonic speeds. A primary consideration has been the prediction of drag for designs which have multiple engines installed in close proximity. New nozzle concepts have been developed which must operate with high performance in the complex flow fields of aircraft afterbody environments. The merging internal and external flow streams result in mutual interactions making theoretical analysis of the associated aerodynamic phenomena most difficult. Because of the large number of variables involved, the performance of complex afterbodies can be accurately estimated only by wind-tunnel or flight experiments (Refs. (1) through (3)).

The purpose of this paper is to examine the mutual aircraft afterbody and engine nozzle aerodynamic interferences. Information was derived from many model experimental investigations of jet interference effects obtained at the National Aeronautics and Space Administration's Langley Research Center at subsonic, transonic, and supersonic speeds.

2. APPARATUS

The material for this paper is drawn from a number of investigations involving a variety of jet-exit testing techniques. Detailed description of the apparatus and techniques is given in the references (i.e., (4) and (5)). Data were obtained principally from strut-supported models at zero angle of attack using cold air or the decomposition products of hydrogen peroxide as the jet fluid. Because of the large number of variables involved, it was felt that, at least for exploratory research, simplicity of the equipment would enhance the reliability of the results. The photograph in Figure 1 shows the air-powered twin-engine dynamometer in the 16-foot transonic tunnel. The circumferential line marks the separation plane between the nonmetric forebody and the metric afterbody. This model incorporates a tandem balance arrangement in which the main balance measured overall thrust minus afterbody plus nozzle drag. A low-capacity balance attached to the main balance measured only forces on the afterbody shell. This system provides a breakdown of engine thrust and afterbody drag as well as jet effects on afterbody drag (Ref. (5)).

In most aircraft configurations, an interface exists at the location from which the exhaust nozzle protrudes from the engine nacelle fairing. Many kinds of exhaust nozzles have been proposed for twin-engine fuselage aircraft; those that will be discussed herein are illustrated in Figure 2. The gap between the airframe afterbody fairing (dotted) and the nozzle (crosshatched) indicates the interface and is similar to the model test installations that were investigated. The upper sketch for each type of nozzle indicates the minimum throat area configuration which will be designated "dry power" in later figures. The lower sketch represents maximum throat area, corresponding to maximum augmented power.

The flap-type convergent nozzle is in the upper left, shown with flaps exposed on top and with the nozzle fully shrouded by the afterbody in the lower sketch. The variable flap convergent-divergent nozzle is in the lower left (Ref. (6)). Three operating modes are illustrated in the center group for the iris translating nozzle (Ref. (7)): minimum throat area on the top sketch, maximum convergent throat area in the center, and maximum throat area with an extensible nozzle shroud on the bottom (similar to nozzle of Ref. (8)). The upper-right sketches are the cone plug concept wherein the nozzle throat area is increased by collapsing the plug. The last two sketches are for the blow-in-door nozzle for the same two power settings (Ref. (2)). For the nozzles on the right, the external flow can affect nozzle internal performance. The external flow over the lip can alter pressures on the plug relative to static performance (Refs. (3) and (9)). The quality of the boundary-layer air and external flow disturbances may affect internal performance of the blow-in-door during dry power operation (Refs. (2) and (10)).

It has generally become accepted practice to include the drag of the nozzle external surfaces as part of the nozzle performance (crosshatched region beyond the interface). The performance parameter that will be presented for the nozzles is the gross thrust at the exit minus the nozzle drag ratioed to ideal isentropic thrust. Secondary flow is not considered in the following results presented, and the special thrust definitions for the blow-in-door nozzle are found in Reference (10).

3. AIRFRAME INSTALLATION EFFECTS ON NOZZLE PERFORMANCE

The prediction of the installed performance of engine nozzles in an airframe can become quite difficult when one realizes the wide variety of propulsion exhaust systems and aircraft designs that may be conceived. Figure 3 is an example of a simplified installation consisting of multiple engines in a closely spaced package. The isolated nacelle shown on the left had a convergent-divergent nozzle with a 5° boattail. The same nozzle configuration in a side-by-side cluster of four engines with circular arc interfairings between them is shown on the right photograph.

3.1 Clustered Jet Exits

In Figure 4 some results from the clustered installation are compared with those for the isolated nozzle. The variation of nozzle performance (gross thrust minus nozzle drag ratioed to isentropic thrust) with Mach number is presented for a typical turbojet pressure ratio schedule. The upper solid line is the performance of the uninstalled isolated nacelle. The short dashed line shows the installed performance for the in-line cluster and the long-short dash curve is for the staggered arrangement. The drag term includes only the pressure drag on the nozzles. The main installation performance penalty occurs at transonic speeds where a decrement of about 2 percent exists. Staggering the two inboard engines had a slight beneficial effect at supersonic speeds because of favorable interference from the outboard jet exhausts on the boattails of the inboard nozzles (Ref. (11)). The low level of performance for this fixed

C-D nozzle is due to comparisons being made for no secondary flow in the ejector whereas it was designed for a corrected weight flow ratio of 0.07 (Ref. (4)).

3.2 Afterbody Boattailing Upstream of Nozzles

In the previous figure on clustered jets, the nozzles all had cylindrical approach sections at the nozzle attachment point. A variable in the design of an aircraft afterbody is the boattail angle upstream of the nozzle station as indicated in the sketch of Figure 5. For these twin-engine afterbodies, maximum cross-sectional area and engine lateral spacing were held constant. The afterbodies incorporated nozzle approach angles of 3°, 6°, and 9°, and the nozzles were of the iris convergent type with throat sizes to simulate dry power, maximum augmentation, and maximum power with shroud extended. Data are presented for jet pressure ratios appropriate to the selected values of Mach number.

The nozzle performance parameter is an increment relative to the nozzle static thrust ratio, F_j/F_i. The shaded regions in the sketches indicate the nozzle surfaces on which the external stream can exert drag or thrust. At $M = 0.8$, pressure recovery in the external airstream exerts a thrust on the nozzle surface which causes the nozzle performance to exceed the static value. This favorable pressure recovery becomes more pronounced as the boattail angle is increased. Similar subsonic trends (decrease in nozzle drag) were found for isolated nacelles by Henry and Cahn some 15 years ago (Ref. (12)). At transonic speeds, approach angle had little effect on the performance. At $M = 2.0$ the nozzle is underexpanded and supersonic jet interference pressurizes the boattailed portion of the shroud, producing a small favorable performance increment at the lowest approach angle. Increasing the approach boattail angle to 9° causes drag on the shroud as a result of lowering the level of pressures.

3.3 Tail Interference on Nozzle Performance

The combined interference of both horizontal and vertical tails on the installed performance of convergent-divergent nozzles in a twin-engine afterbody is illustrated in Figure 6. Data are for a model angle of attack of zero and all tail incidence angles were zero degrees. The plots show the variation of nozzle performance increment (tails on minus tails off) with Mach number. With these nozzles in the dry power setting, for which the nozzle boattail was 14°, the addition of tails to the basic configuration caused a loss in nozzle performance of as much as 4 percent at $M = 0.95$. This loss is due primarily to reduced pressures on the nozzle boattail caused simply by proximity of another aerodynamic body, in this case the tail surfaces. In maximum augmentation this nozzle was almost cylindrical, and addition of the tail surfaces causes slightly favorable interference.

3.4 Afterbody Shaping Effects on Nozzle Performance

The effect of twin-engine installation environment on exhaust nozzle performance is further illustrated in the bar chart of Figure 7 for subsonic dry power and augmented power at Mach numbers of 1.2 and 2.2. The performance parameter is an increment based on the static performance. Convergent, convergent-divergent, conical plug, and blow-in-door nozzles were investigated in combination with two afterbodies which differed in nozzle environment. All nozzles had the same primary throat area for a given power setting. The afterbody designated as "smooth" was more or less idealized with contours which faired well into the nozzle external surfaces and had no base between the nozzles. The afterbody labeled "protrusions" incorporated a fuselage extension between the nozzles and a streamlined extension outboard of each nozzle. These fuselage extensions allowed clearance for changes in nozzle geometry with power settings but were not in physical contact with the nozzles. Performance of the exhaust nozzles in combination with the afterbody with protrusions is indicated by the crosshatched bars, in combination with the smooth afterbody by the open bars.

At subsonic speeds, the smooth afterbody permits pressure recovery to progress to the end of the nozzles, resulting in thrust on the nozzle boattails. The installed performance generally exceeds the static values. The effect of protrusions is to spoil the potential character of the external flow in the vicinity of the nozzles with consequent loss of nozzle boattail thrust. At $M = 0.8$ the installation effect between these two afterbodies for the convergent and convergent-divergent nozzles makes a difference in nozzle performance of about 11 percent of the gross thrust. At transonic speeds, the external flow exerts a pressure drag on the nozzle outer surface and reduces nozzle performance with both afterbodies. At supersonic speeds, the smooth afterbody provides the better operating environment for the nozzles.

The nozzle performance data presented here are not intended for use in nozzle selection, but rather to show generally that all nozzle types are similarly affected by operating environment and preservation of undisturbed external flow over the nozzle boattail leads to improved performance (Ref. (13)).

3.5 Effect of Lateral Spacing on Nozzle Performance

In twin-engine fuselage installations the lateral distance between engines can vary for a number of reasons. To determine the importance of engine spacing on installed nozzle performance, an investigation was conducted on this type of arrangement in which nacelle shape and interfairing shape between the engine nozzles were held constant and three smooth afterbodies of the same length, but varying in width, were utilized. Results of this study are presented in Figure 8. An incremental thrust minus nozzle drag expressed as a ratio to isentropic gross thrust referenced to the static thrust-ratio of each nozzle is again used as a performance indicator. The spacing parameter is the ratio of distance between engine center lines to nozzle maximum diameter. As previously noted, performance values greater than unity were obtained subsonically because of the positive pressure recovery causing thrust on the nozzle boattails.

At $M = 1.2$, with augmented power, the results are similar to those shown in the previous figure, although the data trends for certain nozzles indicate that some improvement in exhaust nozzle performance can be realized by increasing the spacing between the nozzles. However, the effect of lateral spacing of the engines on exhaust nozzle performance is not a major consideration in aerodynamically clean configurations of the type tested.

4. NOZZLE INSTALLATION EFFECTS ON AIRFRAME PERFORMANCE

The previous section has dealt with airframe installation effects on nozzle performance. Turning now to the other aerodynamic interference, that of the jet exhaust flow and nozzle installation effects on the aircraft, the discussion will be mainly concerned with the drag of the afterbody-nozzle combination and interference on aerodynamic and stability characteristics.

4.1 Effect of Jet-Exit Axial Location on Afterbody Drag

Engine-exhaust system installations in a fuselage provide many options for axial and lateral locations. The axial position depends on a trade between propulsion system weight and aircraft balance and the influence of the jet exhaust on vehicle performance, stability, and induced structural loading (Refs. (1) and (14)). The problem of axial location of jet exits in an afterbody arrangement was given elementary treatment in a study (Ref. (5)), which is illustrated by the sketches in Figure 9, for afterbodies of equal size and overall length. The circular symbols indicate the jet exits located at the extreme aft end, the square symbols indicate the exits moved forward by one-half body width, and the diamond symbols indicate exits moved forward by one full body width upstream of the wedge apex.

The results show the variation with Mach number of afterbody drag coefficient (based on A_{max}) with the jets operating at values of pressure ratio appropriate to Mach number for a turbofan engine. Because drag is measured on only the aft portion of a complete body, the absolute values are not pertinent; however, the differences in afterbody drag coefficient are significant. The dashed curve shows calculated drag coefficient for an axisymmetric afterbody having the same axial distribution of cross-sectional area as the afterbody having extreme aft location of the exits. Actually, all the afterbodies have the same basic Haack-Adams shape when the jets are cylindrical. At subsonic speeds, the configuration with exits at the extreme aft end has the lowest level of drag, and afterbody drag increases as length of the interfairing is increased. This order of excellence is maintained at speeds up to a Mach number of about 1.3. At higher supersonic speeds, favorable interference of the jet plume reduces the drag of all configurations, but the afterbodies having extended interfairings are better adapted to derive benefit from this effect (Ref. (15)).

4.2 Engine Lateral Spacing Effect on Afterbody Drag

Results from two lateral spacing investigations will be presented for which simplified clean afterbodies were studied with the same forebody and support system shown in Figure 1. Both maximum cross-sectional area and nozzle throat areas were kept constant for a given power setting. Each type of nozzle installation had the same axial distribution of cross-sectional area and the same fineness ratio for the two lateral spacings.

Figure 10 depicts results for a flap-type convergent nozzle in afterbodies with close and wide lateral spacings. For these configurations, the convergent nozzles were not exposed to the airstream; the drag includes the force on the afterbody shroud and the nozzle annulus base drag, as in the previous figure. Drag coefficients are shown for spacing ratios based on the jet diameter, d_t, at each power setting. Afterbody drag generally increases with spacing ratio except for the anomaly at $M = 0.8$ with dry power where the close-spaced jets influence the base region. Drag would increase with spacing ratio in all cases if only the forces on the shroud alone are considered.

During this investigation the basic interfairing, which was faired to a horizontal sharp edge just ahead of the exit, was altered to form a blunt base interfairing by a flat fairing over the gulley between the tailpipe nacelles. Power effects on pressures measured on the flat base between the exits for the close-spaced configuration are exhibited in Figure 11. The symbols indicate locations of pressure orifices on the slightly recessed afterbody base. At $M = 0.8$ considerable variation in base pressure cofficient occurred, depending on location, which was also true at $M = 1.2$ for dry power. For normal operating jet pressure ratios at these speeds, drag exists on the base. At $M = 2.2$ the pressure is constant over the base and a slightly favorable force can result. These results are similar to those of Reference (13) but in contrast with data obtained on a model having a higher degree of afterbody boattailing (Ref. (16)).

Lateral spacing results are shown on Figure 12 for afterbodies with convergent-divergent nozzles where the drag coefficients represent combined drag of the afterbodies and nozzles. These afterbodies with close and wide lateral spacing were designed with the same constraints as the previous series, and data for models having a basic streamline interfairing are shown. The spacing ratio s/d_e is referenced to nozzle exit diameter which was closed down for dry power ($\beta = 18^\circ$) and opened to a cylindrical external shape for augmented conditions. The drag increases slightly with spacing ratio for all speed and power settings. The results of Figures 10 and 12 indicate that for the clean type of twin-engine afterbody, lateral spacing of the engines does not have a large effect on afterbody-nozzle performance.

4.3 Interfairing Shape Influence on Afterbody Plus Nozzle Drag

The shape of the interfairing between the engine nacelles can influence the drag of the afterbody, nozzles, or combination of afterbody and nozzles, depending on the termination point of the interfairing relative to the nozzles (Refs. (11) and (13)). Figure 13 presents results on varying the interfairing shape for a closely spaced twin-jet afterbody configuration which had a 3° approach boattail angle to the nozzles. The three-position iris nozzle (Fig. 2) was tested in combination with several afterbody interfairings. Three interfairing shapes which terminated at the afterbody-nozzle interface were studied: a circular arc, an elliptical, and a blunt (flat base) configuration. In addition, an extended interfairing which was a continuation of the blunt configuration was utilized and this interfairing terminated downstream of the longest nozzle in a small flat base. The variation of drag coefficient for afterbody plus nozzles with Mach number for a typical jet pressure ratio schedule is given on the figure. The upper-left plot shows data for the dry power iris convergent nozzle. The lower-left data points are for the augmented iris nozzle configuration, as are the open symbols shown at transonic speeds. The solid symbols represent the augmented shrouded nozzle with the elliptical and extended interfairings. The elliptical interfairing

provides the lowest drag for the unshrouded nozzles as shown by the dashed lines (similar to results in Ref. (11)). The difference in afterbody plus nozzle drag between the blunt and elliptical interfairings for dry power represents an increase in drag coefficient of about 40 percent. For the augmented iris, the difference in drag coefficient for the same two interfairings is about 30 percent. At transonic speeds, small differences exist for the various interfairings. The shrouded augmented iris nozzle which had less boattailing was tested at supersonic speeds. An opposite trend is noted for the extended interfairing at these speeds as it now has the lowest drag. This has been observed previously (Refs. (5), (13), and (15)) where a pluming jet can pressurize aft sloping surfaces, but the extended interfairings generally have a detrimental effect on performance at subsonic speeds.

4.4 Interference Effects on Aircraft Aerodynamics

The discussion to this point has dealt with interferences on afterbodies incorporating the exhaust nozzles. Attention is now directed to jet interference effects on the complete aircraft aerodynamics. The testing techniques for complete powered models are usually more difficult because of support system and inlet simulation problems. Shown in Figure 14 is a sketch of a single-engine four-jet V/STOL-type aircraft. The exhaust nozzles, two on each side, are located close beneath the wing. The data represent the change in aerodynamic coefficients caused by change from power-off to power-on flight. Results are shown as a function of angle of attack for $M = 0.8$ and horizontal-tail deflections of 0° and 5°. In this case, jet effects are not large. Jet operation decreased lift and drag and increased pitching moment. When referred to absolute values of the coefficients required in flight, these increments represent a reduction in lift and drag, respectively, of about 5 and 10 percent. Although the magnitude of pitching-moment coefficient increased due to simulated jet operation, only slight changes in the model longitudinal stability were found. Additional aspects of jet exhaust interference on airframe characteristics are presented in References (1) and (17).

5. CONCLUDING REMARKS

A review of exploratory studies of simplified afterbody-nozzle combinations has pointed out many of the variables affecting the aerodynamic interferences between the exhaust system and the airframe. Experimental data presented have shown that aerodynamic refinement of the exhaust nozzle installation is of primary importance. Obstruction or disturbance of the potential nature of the external flow by airframe components in proximity to the exhaust nozzles generally leads to increased drag of the nozzle boattail and to degraded performance of the aircraft. In twin-engine aircraft with engines mounted in the aft fuselage, lateral spacing of the engines does not appear to be a major design consideration. For aircraft having missions primarily at subsonic speeds, best performance was obtained with exhaust nozzles forming the downstream terminus, and moderately large approach boattail angles may be used without adverse effects on overall performance. For best performance of a supersonic aircraft, nozzle approach boattail angle should be kept to a small value, and a downstream extension of the fuselage between the nozzles may be advantageous.

Each of the components and design features that have been examined contribute an individual interference on the airframe-nozzle installation. Obviously, real aircraft designs will incorporate many of these arrangements in combination and will be subject to additional variables such as deflection of aircraft surfaces and attitude effects, all of which will make the back end flow field even more complex. Therefore, detailed simulation of the complete aircraft model and internal flows is required to provide the proper environment in the wind tunnel for prediction of installed nozzle performance and afterbody drag.

REFERENCES

(1) Nichols, Mark R. — Aerodynamics of Airframe-Engine Integration of Advanced Supersonic Aircraft. Gas Turbines, AGARD Conference Proceedings Series No. 9, Part I, 1966. NASA TN D-3390, Aug. 1966.

(2) Motycka, D. L.; Skowronek, P. J., Jr. — Performance Installation Effects for Nozzles Installed on a Twin-Jet Fighter Airplane Model. Paper presented at the Society of Automotive Engineers Meeting, April 29-May 2, 1968. SAE Preprint 680296.

(3) Beheim, Milton A.; Boksenbom, Aaron S. — Variable Geometry Requirements in Inlets and Exhaust Nozzles for High Mach Number Applications. Paper presented at Sixth Congress of the International Council of the Aeronautical Sciences. Sept. 9-13, 1968. NASA TM X-52447.

(4) Norton, Harry T., Jr.; Pendergraft, Odis C., Jr. — Transonic Performance of a Convergent-Divergent Ejector Nozzle Designed for a Corrected Secondary-Weight Flow Ratio of 0.07. NASA TM X-974, June 1964.

(5) Berrier, Bobby Lee; Wood, Frederick H., Jr. — Effect of Jet Velocity and Axial Location of Nozzle Exit on the Performance of a Twin-Jet Afterbody Model at Mach Numbers Up to 2.2. NASA TN D-5393, Sept. 1969.

(6) Ammer, R. C.; Punch, W. F. — Variable-Geometry Exhaust Nozzles and Their Effects on Airplane Performance. Paper presented at the Society of Automotive Engineers Meeting, April 29-May 2, 1968. SAE Preprint 680295.

(7) Greathouse, William K. — Blending Propulsion With Airframe. Space/Aeronautics, Vol. 50, No. 6, Nov. 1968, pp. 59-68.

(8) Valerino, Alfred S.; Yeager, Richard A. — External-Stream Effects on Gross Thrust and Pumping Characteristics of Ejectors Operating at Off-Design Mach Numbers. NACA RME56C14, June 1956.

(9) Berrier, Bobby L. — Effect of Plug and Shroud Geometry Variables on Plug-Nozzle Performance at Transonic Speeds. NASA TN D-5098, March 1969.

(10) Laughrey, James A. — Calculation of the Performance of Installed Exhaust Nozzles on Supersonic Aircraft. Paper No. 69-428 presented at AIAA Propulsion Joint Specialist Conference, Colorado Springs, Colorado, June 9-13, 1969.

(11) Kirkham, Frank S. et al. — Afterbody Drag of Several Clustered Jet-Exit Configurations at Transonic Speeds. NASA TM X-1216, March 1966.

(12) Henry, Beverly Z. Cahn, Maurice S. — Additional Results of an Investigation at Transonic Speeds to Determine the Effects of a Heated Propulsive Jet on the Drag Characteristics of a Series of Related Afterbodies. NACA RML56G12, Sept. 1956.

(13) Migdal, D. et al. — An Experimental Evaluation of Exhaust Nozzle/Airframe Interference. Paper No. 69-430 presented at AIAA Propulsion Joint Specialists Conference, Colorado Springs, Colorado, June 9-13, 1969.

(14) Cornette, Eldon S. Ward, Donald H. — Transonic Wind-Tunnel Investigation of the Effects of a Heated Propulsive Jet on the Pressure Distribution Along a Fuselage Overhang. NACA RML56A27, April 1956.

(15) Pitts, William C. Wiggins, Lyle E. — Axial-Force Reduction by Interference Between Jet and Neighboring Afterbody. NASA TN D-332, Sept. 1960.

(16) Langfelder, Helmut — Low-Drag Installation of Twin-Propulsion Nozzles in the Rear of the Fuselage for Transonic and Supersonic Flight. Aerodynamics of Power Plant Installation, Part I, AGARDograph 103, Oct. 1965, pp. 195-216.

(17) Henry, Beverly Z., Jr. — Interference Effects at Transonic Speeds of Jets Exhausting From the Hull Step of a Model of a Large Water-Based Airplane. NASA TM X-218, Jan. 1960.

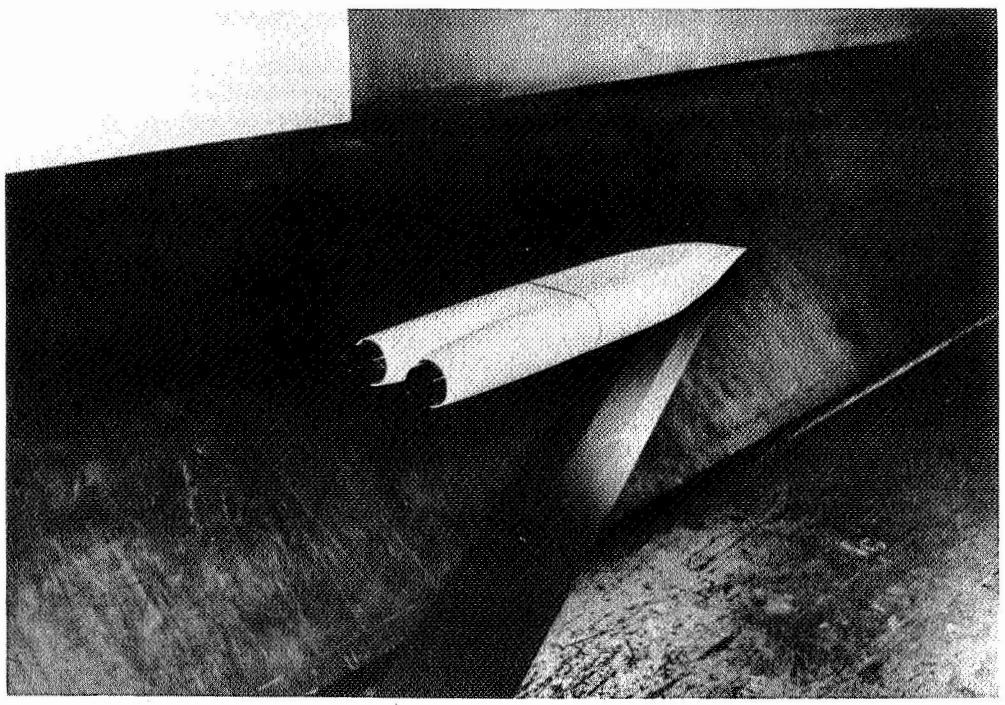

Fig.1 Twin-engine afterbody-nozzle model

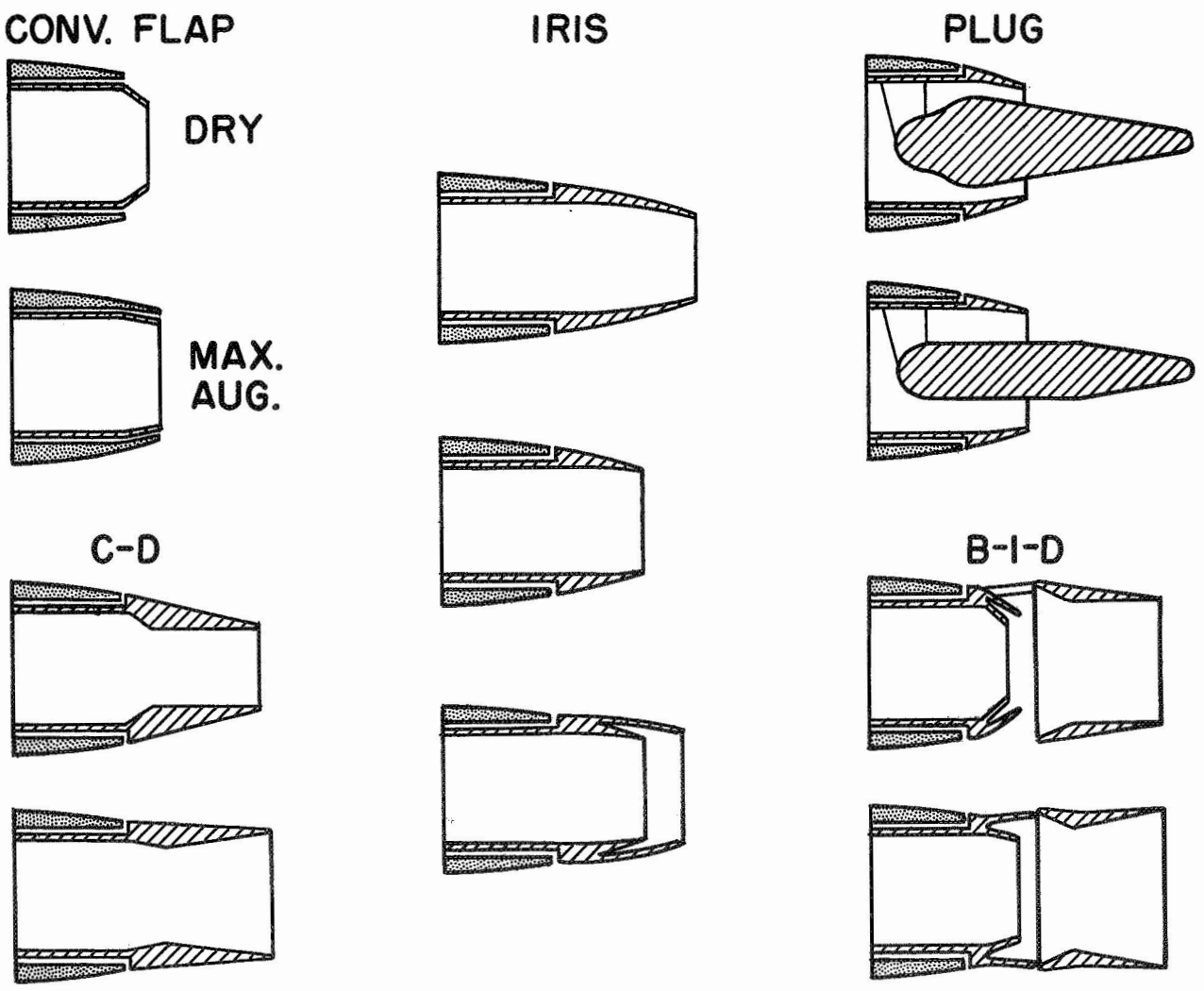

Fig.2 Nozzle types. Minimum and maximum throat areas

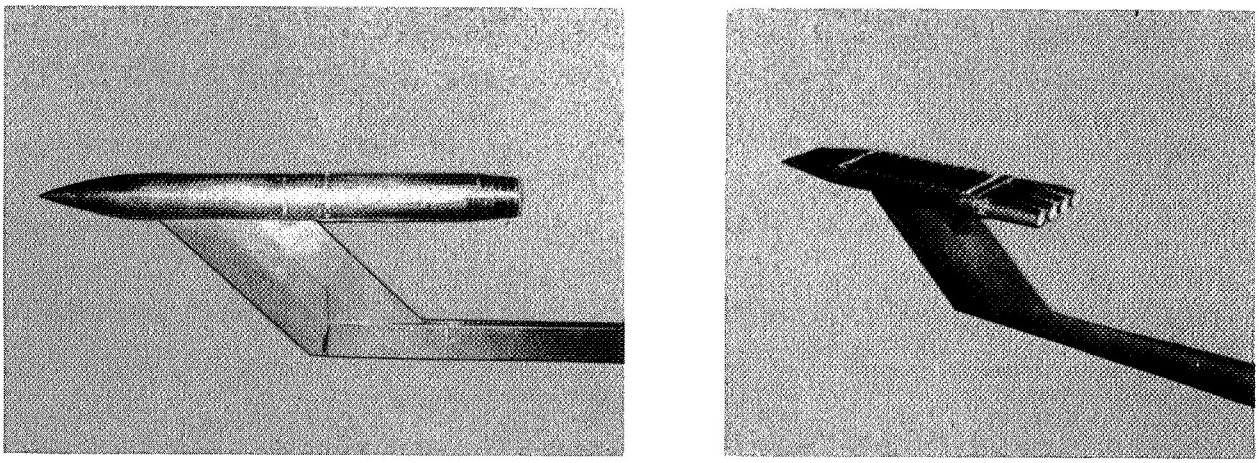

Fig.3 Clustered jet installation.

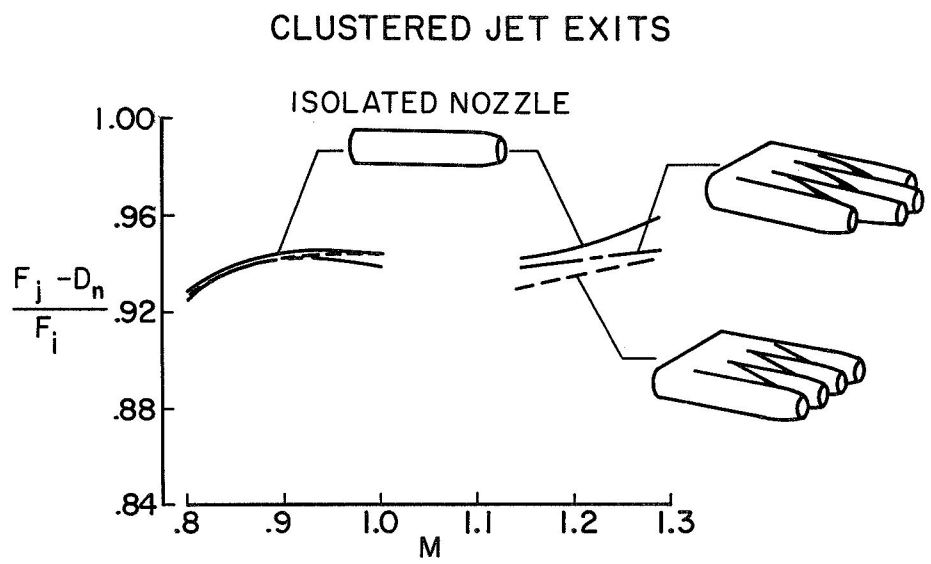

Fig.4 Installed nozzle performance

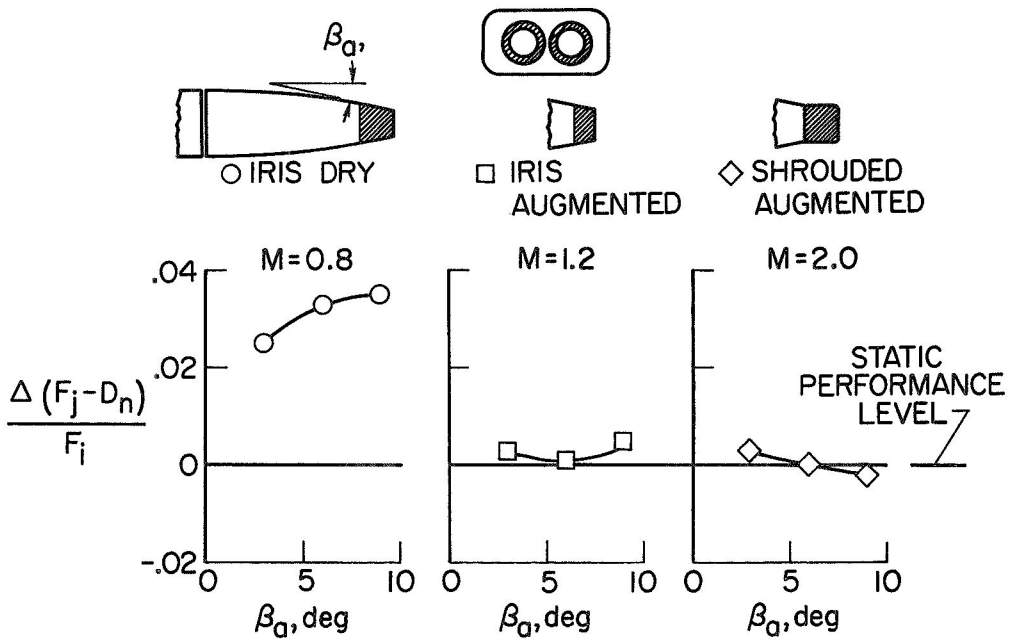

Fig.5 Effect of afterbody approach angle on nozzle performance

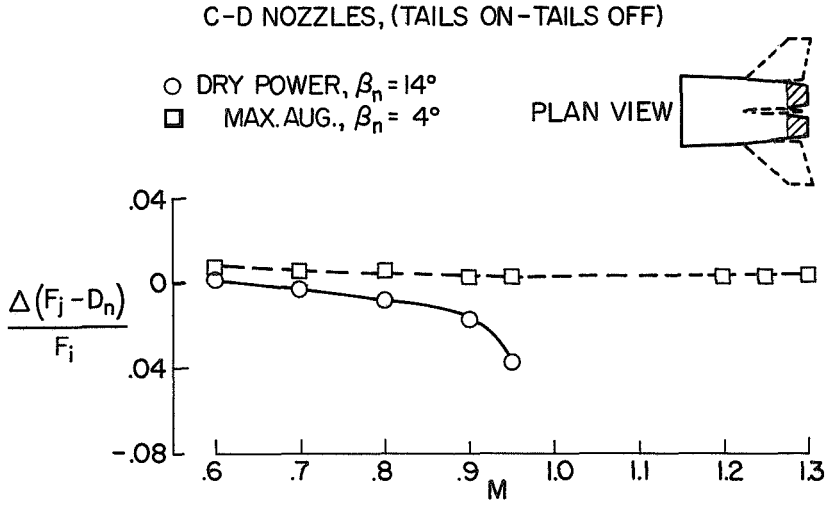

Fig.6 Tail interference on nozzle performance

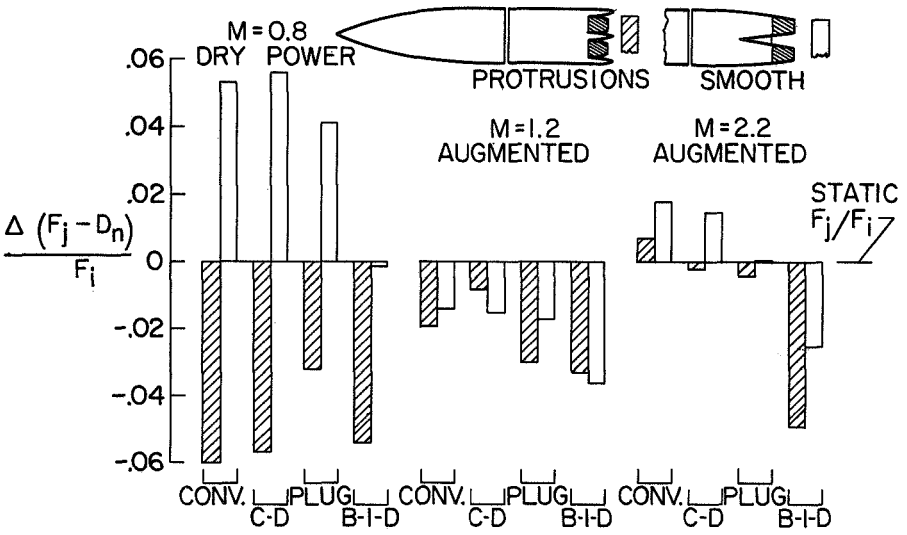

Fig.7 Afterbody shaping effects on nozzle performance

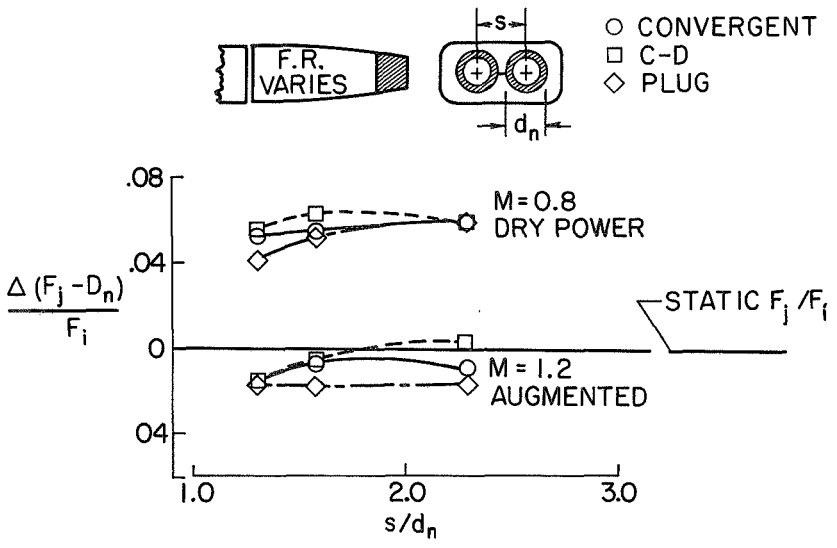

Fig.8 Effect of lateral spacing on nozzle performance

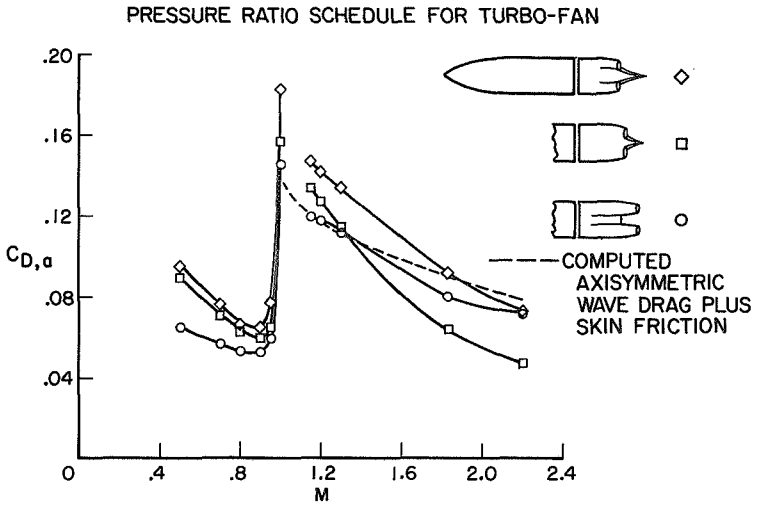

Fig.9 Effect of jet-exit axial location on afterbody drag

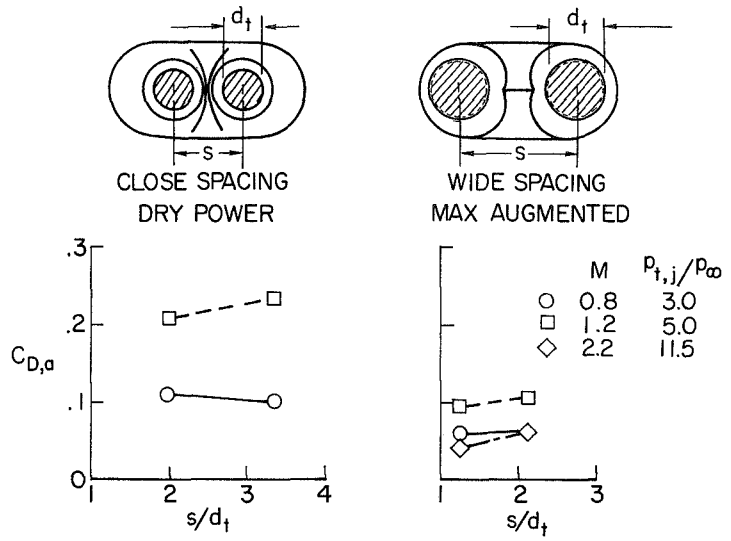

Fig.10 Effect of engine spacing on afterbody drag of a model with convergent nozzles

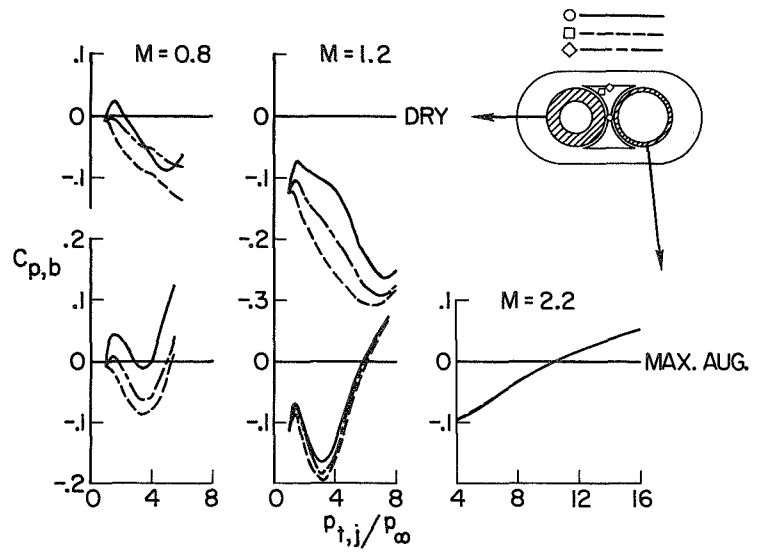

Fig.11 Jet effects on afterbody base pressure coefficients

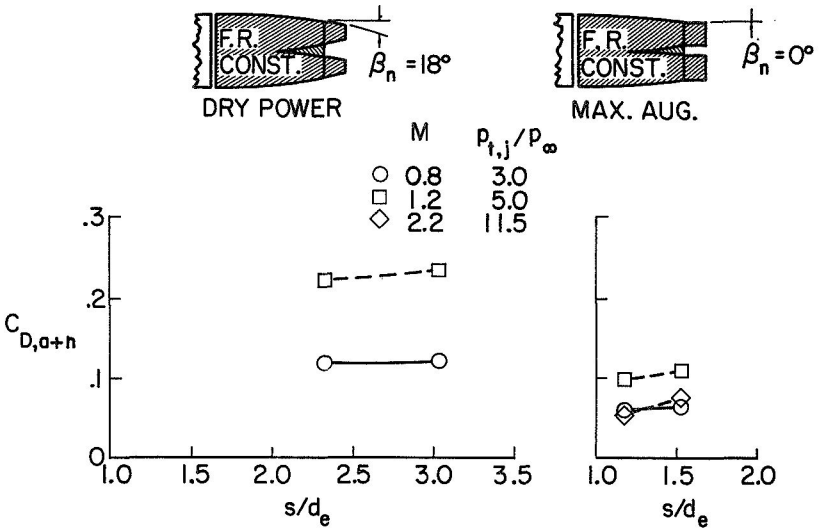

Fig.12 Effect of engine spacing on drag of afterbody plus nozzles for model with convergent-divergent nozzles

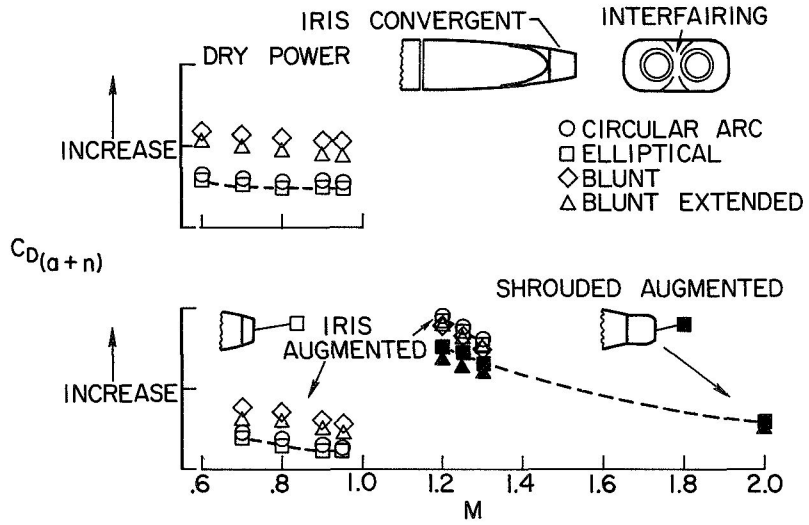

Fig.13 Interfairing shape influence on afterbody plus nozzle drag

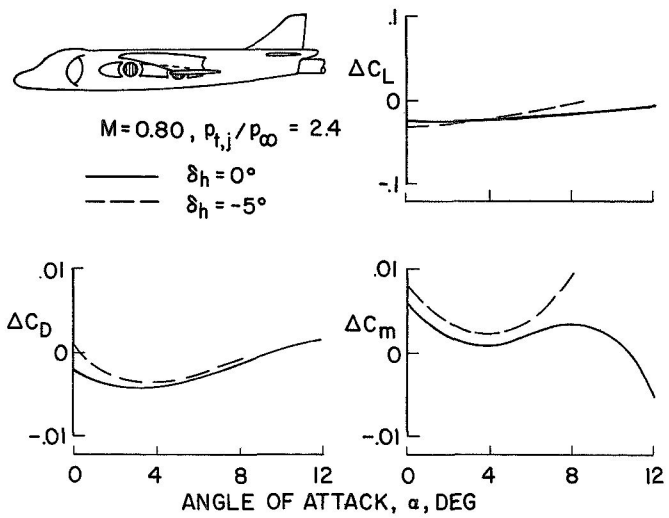

Fig.14 Jet effects on aerodynamic characteristics of a four-jet V/STOL model.